*J. Electrochem. Sci. Eng.* **13(3)** (2023) 575-588; http://dx.doi.org/10.5599/jese.1721

Open Access : : ISSN 1847-9286
www.jESE-online.org

*Original scientific paper*

# One-pot synthesis of crystalline structure: Nickel-iron phosphide and selenide for hydrogen production in alkaline water splitting

Mukhtiar Ahmed[1,✉], Abdul Hanan[2], Muhammad Nazim Lakhan[2,✉], Altaf Hussain [3,4] Irfan Ali Soomro[5], Binguang Niu[1], Yang Yang[1]

[1]*State Key Laboratory of Multiphase Complex Systems, Institute of Process Engineering, Chinese Academy of Sciences, University of Chinese Academy of Sciences, Beijing 100190, China*
[2]*Key Laboratory of Superlight Material and Surface Technology, Ministry of Education, College of Materials Science and Chemical Engineering, Harbin Engineering University, Harbin 150001, China*
[3]*State Key Laboratory of Electroanalytical Chemistry, Changchun Institute of Applied Chemistry, Chinese Academy of Sciences, Changchun 130000, China*
[4]*University of Science and Technology of China, Hefei, Anhui, China*
[5]*College of Chemical Engineering, Beijing University of Chemical Technology, Beijing 100190, China*

*Corresponding authors:* ✉ahmedmukhtiar461@gmail.com; ✉nazimlakhan@gmail.com

Received: February 21, 2023; Accepted: June 22, 2023; Published: June 27, 2023

***Abstract***

*Electrocatalytically active nanocomposites play a vital role in energy generation, conversion, and storage technologies. Transition metal-based catalysts such as nickel and iron and their pnictide (phosphide), and chalcogenide (selenide) compounds exhibit good activity for hydrogen evolution reaction (HER) in the alkaline environment. In this study, transition metals-based catalysts (Ni-P-Se, Fe-P-Se, and Ni-Fe-P-Se) solutions were prepared using a simple one-pot method. Prepared solutions were deposited on Ni foam, and different characterization techniques were used to determine the composition, structure, and morphology of as-prepared catalysts. Furthermore, it was found that Ni-Fe-P-Se as a cathode material showed better HER performance compared to other investigated materials with the overpotential value of 316 mV at 10 mA $cm^{-2}$ current density and 89 mV $dec^{-1}$ Tafel slope value. The stability tests of the as-prepared catalyst confirmed that the synergistic effect between various elements enhances the electrocatalytic performance for up to 24 hours, providing a fair, stable nature of Ni-Fe-P-Se based sample.*

**Keywords**

Electrocatalysis; hydrogen evolution reaction; transition metal phosphide; transition metal selenide

## Introduction

Developed nations have made a commitment to switching over immediately to environmentally friendly electrochemical energy. Renewable energy sources like wind and solar energy are crucial in

order to reduce the use of fossil fuels and environmental degradation. Electrochemical water splitting (EWS) is one of the most promising strategies that can be used to address energy issues due to its purity, safety, and ease of use [1,2]. EWS includes two half-cell reactions, such as hydrogen evolution reaction (HER) and oxygen evolution reaction (OER). Both the anodic and cathodic reactions result in the creation of hydrogen and oxygen, respectively [3,4]. In addition, several studies have focused not only on the production of new catalysts but also on the discovery of new affordable fuels. In this regard, particular attention has recently been paid to hydrogen fuel, which has been suggested as the secondary energy source for the future [5-7].

Among noble metals, platinum-based catalysts are the most active for HER. However, the high price and resource shortage of noble metal electrocatalysts limit their application in water splitting application. To address this problem, scientists began to explore earth-rich transition metals (TMs) to replace precious metal-based catalysts. Transition metal phosphide and selenide (TMP/TMSe) have got a lot of interest due to their flexibility in a variety of applications, such as catalysts, batteries, and supercapacitors [8-10]. There have been several efforts to produce a less expensive composite material that can replace noble metals for hydrogen production. According to previous studies, TMP/TMSe have been synthesized through one-pot processes resulting in highly active catalysts [11-14]. Nickel (Ni) and iron (Fe) TM alloys were also considered efficient materials owing to their exceptional properties, such as hardness and conductivity. Therefore, preparing Ni and Fe composites with P and Se could be a valuable approach for hydrogen production. For example, Pei *et al.* [15] developed a series of highly active and inexpensive Co–Ni–P films by a one-step constant current density electrodeposition method. These films were demonstrated to be efficient bifunctional catalysts for both $H_2$ and $O_2$ evolution (HER and OER), while deposition time was deemed the crucial factor governing electrochemical performance. In particular, it requires −103 mV overpotential for HER and 340 mV for OER to achieve the current density of 10 mA $cm^{-2}$, corresponding Tafel slopes of 33 and 67 mV $dec^{-1}$, respectively. Xu *et al*. [16] fabricated the Fe–Co–P multi-heterostructure arrays consisting of CoP, $Co_2P$ and FeP, built for water splitting by a self-sacrificial template method. Such multi-heterostructures adjust the local electronic structure and then improve the adsorption of reaction intermediates on active sites, which was further proved through density functional theory (DFT) calculations. Xing *et al.* [17] fabricated a unique 2D $FeSe_2$/CoSe nanosheet structure synthesized by hydrothermal and selenization processes. In an alkaline solution, $FeSe_2$/CoSe nanosheet electrode exhibited a low overpotential of 73 mV at 10 mA $cm^{-2}$ for the HER. Kwak *et al.* [18] reported the synthesis of $CoSe_2$ and $NiSe_2$ nanocrystals (NCs) as excellent bifunctional catalysts for the simultaneous generation of $H_2$ and $O_2$ in water-splitting reactions. $NiSe_2$ NCs exhibited superior electrocatalytic efficiency in OER, with a Tafel slope of 38 mV $dec^{-1}$ (1 M KOH) and HER with 44 mV $dec^{-1}$ (0.5 M $H_2SO_4$). One-pot method is considered advantageous over traditional multi-step synthesis methods, as it reduces the number of reaction steps and the amount of waste generated. It also has the potential for scalability and lower cost [19,20]. This novel one-pot method is offering inherent advantages such as step economy, operational simplicity, and synthetic efficiency.

Herein, Ni and Fe-based P and Se composites such as Ni-P-Se, Fe-P-Se, and Ni-Fe-P-Se were prepared by using the one-pot synthesis method and Ni-foam (NF) was used as a substrate. The as-prepared composites were firstly characterized physically by different techniques, including XRD, SEM, EDS, and HRTEM, for their crystallographic analysis, surface features, elemental presence and deeper morphological aspects, respectively. After that, the as-prepared materials were analysed for HER response in an alkaline medium. The obtained physicochemical and electrochemical outcomes

demonstrated that the Ni-Fe-P-Se could be considered as a prominent electrocatalyst for HER in the alkaline medium.

## Experimental

### *Chemicals*

The experimental procedure involved the use of Ni foam (NF), which was supplied by Sigma-Aldrich. The Ni foam used had a high purity of 99.9 % and a specific surface area ranging from 0.5 to 3 $m^2$ $g^{-1}$. Additionally, the foam had a pore size of around 100-200 micrometres, commonly used in electrochemical applications. The 2-mercaptoethanol with a purity of 93.4 % was provided by Tianjin Guangfu Fine Chemical Research Institute. Selenium (Se) powder with a purity of 97 % was purchased from Sinopharm chemical reagents Co. LTD. Sodium dihydrogen phosphate ($NaH_2PO_4$) was purchased from Tianjin Yaohua chemical reagents Co. LTD, and nickel(II) nitrate $Ni(NO_3)_2{\cdot}6H_2O$ was obtained from Sinopharm chemical reagents Co. LTD. All chemicals used in the synthesis process were of analytical grade. The chemicals were added to the reaction without further treatment, ensuring that the experimental conditions were consistent and reliable.

### *Preparation of Ni-P-Se, Fe-P-Se and Ni-Fe-P-Se materials*

In a typical experimental procedure, commercially purchased chemicals were taken into a mixture with $Ni(NO_3)_2{\cdot}6H_2O$ (1.45 g), $Fe(NO_3)_3$ (1.40 g), $NaH_2PO_2$ (2.00 g), and selenium (Se) (1.2 g) were mixed to prepare different solutions. Ni-P-Se, Fe-P-Se and Ni-Fe-P-Se were prepared, dissolved separately in 35 mL distilled water (DW), and stirred for one hour to form clear solutions. Later, the obtained solutions were centrifuged and washed several times with DW and ethanol for 10 minutes. The centrifuged products, such as Ni-P-Se, Fe-P-Se and Ni-Fe-P-Se, were collected and dried in a vacuum oven overnight at 70 °C. Finally, the dried products were placed in a furnace for annealing under a nitrogen atmosphere. The furnace was heated at 400 °C for 3 hours with a heating rate of 5°C $min^{-1}$. After cooling down the samples (Ni-P-Se, Fe-P-Se and Ni-Fe-P-Se) at room temperature, the as-obtained powder samples were collected and used for further characterizations and electrochemical analysis. The schematic procedure of samples preparation is depicted in Figure 1.

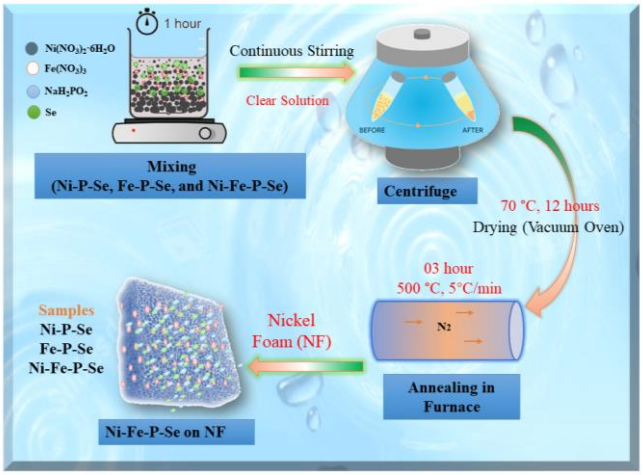


***Figure 1.*** *Schematic illustration of the step-by-step synthesis process of investigated materials*

### *Structural characterizations*

The X-ray diffraction (XRD) patterns were observed by using X-Ray diffractometer (XRD, Rigaku TTR-III) operated at 40 kV/150 mA with high-intensity Cu Ka radiation ($\lambda$ = 0.15406 nm). Transmission

electron microscopy (TEM, Tecnai-G220S-Twin, FEITEM) was used to check the samples' topography and interplanar analysis at 120 kV an accelerating voltage. The corresponding d-spacing value has been calculated through Image-J software (*via* HRTEM images). The morphology and structure of the samples were characterized by scanning electron microscopy (SEM, JSM-6480A, JOEL) run at 20 kV an accelerating voltage and used to determine the shape and structure of the deposited materials on Ni-foam. For deposition, a dispersed solution of binder and the as-prepared catalyst was dispersed on NF *via* drop casting. EDS (energy dispersive x-ray spectroscopy) mapping attached with SEM was used for the confirmation of present elements. This information helped us to optimize their synthesis methods and improve the properties of the resulting materials.

*Electrocatalytic measurements*

Electrocatalytic measurements of HER were conducted by using the traditional three-electrode workstation (CHI760E) bought from Shanghai Chenhua Instrument Co. Ltd. A platinum rod electrode was used as the counter electrode, while a silver silver-chloride (Ag/AgCl) filled with 3.0 M KCl served as the reference electrode. The Pt rod electrode is often used as a counter electrode because it is inert and does not participate in the chemical reactions taking place in the electrochemical cell. As-prepared samples were deposited separately on NF (1×1cm) pieces and used as working electrodes. In 1.0 M KOH, all potentials were calibrated to the reversible hydrogen electrode (RHE) using the Nernst equation and all electrochemical experiments were performed at room temperature. First, 5 mg of each catalyst solution dissolved in 1 mL of DW and 50 mL of 5 % Nafion solution (as a binder) were individually added for catalyst ink preparation. Then, the catalyst ink was properly dispersed using an ultrasonic bath for 20 minutes. Later, 10 mL of dispersed solution was coated by drop casting on NF foam and dried at room temperature. The loaded mass of each catalyst was about 0.2 mg $cm^{-2}$. The electrocatalytic activity for HER was investigated in 1.0 M KOH through the linear sweep voltammetry (LSV) at 5 mV $s^{-1}$ scan rate. KOH is a strong base and can provide a high-conductivity solution, making it a good choice for many electrochemical applications, including HER [21,22].

All potentials measured by Ag/AgCl reference electrode ($E_{Ag/AgCl}$) were converted to the potential of reversible hydrogen electrode ($E_{RHE}$) using equation (1):

$$E_{RHE} = E_{Ag/AgCl} + 0.059pH + E^{\circ}_{Ag/AgCl} \quad (1)$$

where $E^{\circ}_{Ag/AgCl}$ is equal to 0.21 V.

The electrode overpotential ($\eta$) in the HER region is defined as the difference between $E_{RHE}$ and standard equilibrium potential for $H^+/H_2$ (0.00 V), resulting in $\eta = E_{RHE}$.

The Tafel slope, on the other hand, was computed using the Tafel equation (2).

$$\eta = b \log j + a \quad (2)$$

where the overpotential is $\eta$, the Tafel slope is $b$, and the current density is $j$.

The current-time curve is required for assessing the performance of electrocatalyst for HER because it gives essential information on the catalyst efficiency, kinetics, and long-term stability. Based on a particular current level, a current-time curve displays the interrupting time of an overcurrent device, all tests were carried out in an electrocatalysis cell. Preliminary studies revealed that a little adjustment in V had no discernible effect on the current-time curves in the cell. In other words, the small adjustments did not affect the current-time curves in the cell. If significant modifications are made, the current-time curves are likely to be altered [23]. The proposed mechanism of HER on Ni-Fe-P-Se is presented in Figure 2.

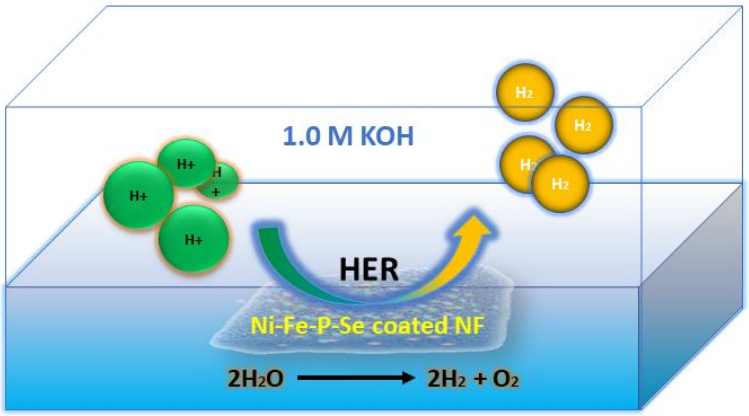


***Figure 2.*** *Proposed mechanism of HER on Ni-Fe-P-Se coated on NF in alkaline media*

## Results and discussion

*Physicochemical analysis*

The X-ray diffraction has been applied to analyse the crystallographic characteristics of various materials, including Ni-P-Se, Fe-P-Se, and Ni-Fe-P-Se, and results are shown in Figure 3.

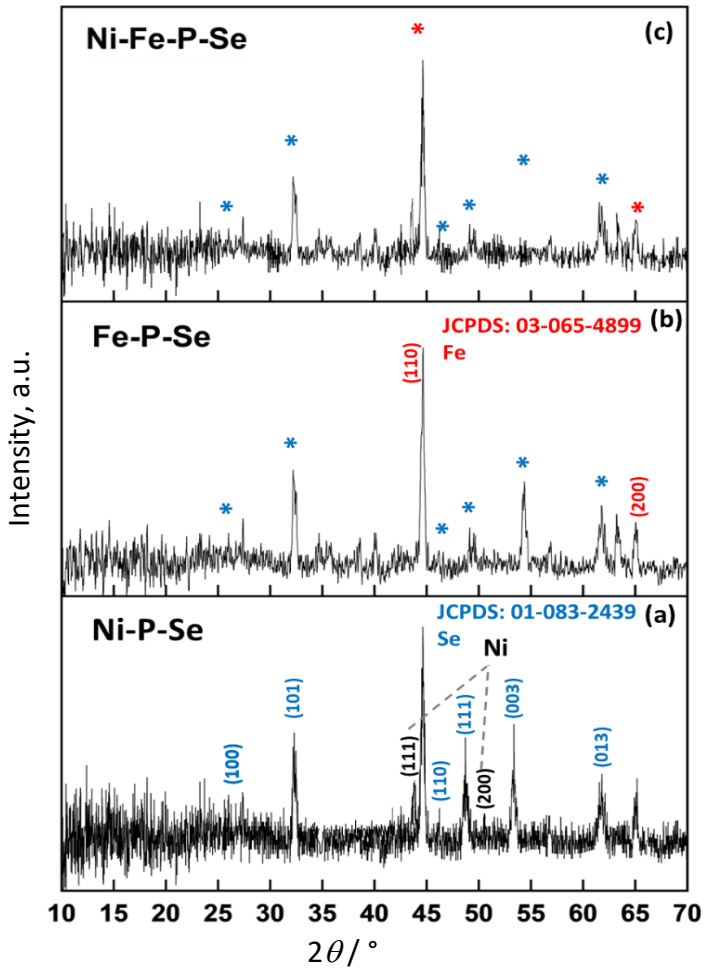


***Figure 3.*** *XRD patterns of corresponding electrocatalytic materials: (a) Ni-P-Se, (b) Fe-P-Se, (c) Ni-Fe-P-Se*

Figure 3a exhibits the Ni-P-Se with a number of diffraction patterns at two theta angles like 26.3, 31.8, 46.5, 49.8, 54.2, and 61.8°, which correspond to the crystallographic planes (100), (101), (110), (111), (003) and (013), having a JCPDS no. 01-083-2439 which resembles the Se presence [24]. Two peaks that have been observed at around 44.1 and 51.3° correspond to (111) and (200)

crystallographic planes and strongly justify the existence of Ni within the as-prepared composite material [25,26]. Fe-P-Se diffraction patterns can be seen in Figure 3b, revealing the presence of Se with additional peaks for iron (Fe) at 44.3 and 65.1° that are attributed to the (110) and (200) crystal planes, having a JCPDS card no. 03-065-4899, which is entirely supported by existing research [27,28]. X-ray patterns of Ni-Fe-P-Se shown in Figure 3c resemble the existence of Ni, Fe, and Se elements. Such findings through XRD analysis confirmed the successful preparation of Ni-Fe-P-Se composition, and this combination of three different elements was already shown to promote the synergistic effect toward HER performance [29,30].

HRTEM is one of the most advanced analytical imaging measurement techniques to distinguish the size and shape of as-prepared samples [31]. In Figure 4a-4c, the images perfectly reflect the detailed morphology of the as-prepared material with the scale bars of 500, 200 and 10 nm, respectively. The HRTEM image for the synthesized material Ni-Fe-P-Se (Figure 4) reveals an uneven surface and different domains resulting from the tight aggregation of nanoparticles with a well-resolved lattice fringes space assigned to the plane of Ni-Fe-P-Se [32]. Figures 4a and 4b illustrate the different magnifications of the samples. The lattice fringe, along with their planner distance measurement, is depicted in Figure 4c, and its fast Fourier transform (FFT) conversion can be found on the right side of the image. The d-spacing value for as-prepared Ni-Fe-P-Se is calculated as 0.221 nm, which is well-matched with recently reported research [33].

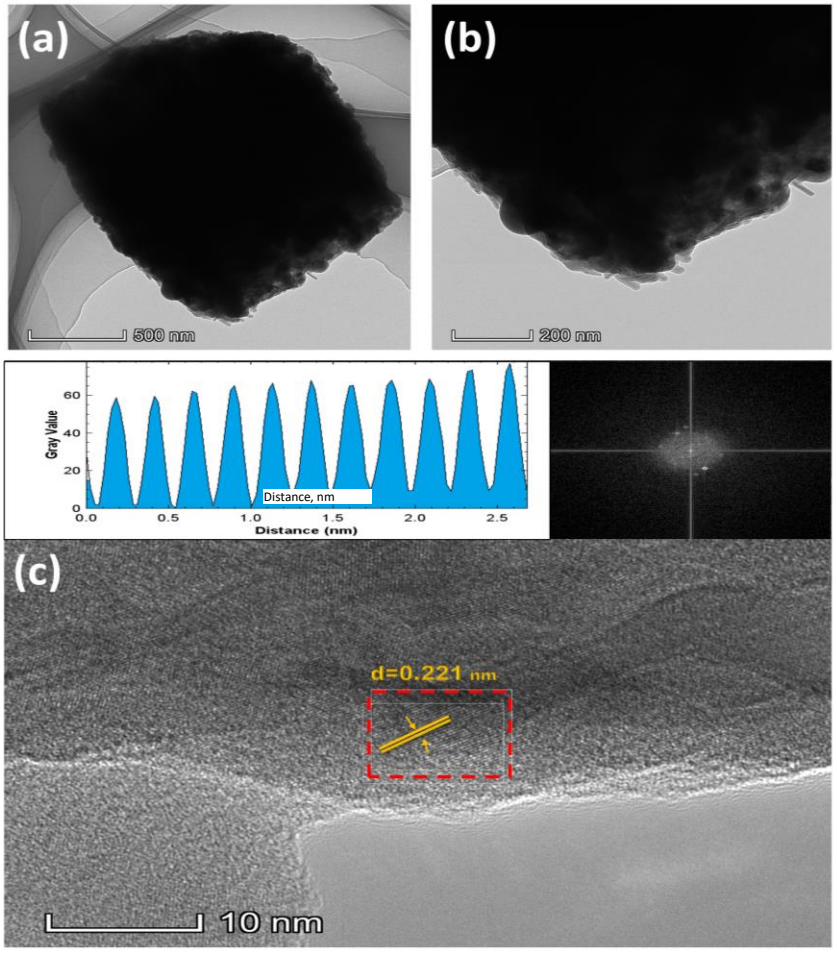


***Figure 4.*** *(a-b) HRTEM images of Ni-Fe-P-Se at different magnifications; (c) lattice fringes and corresponding FFT images for d-spacing calculation*

Figure 5 presents the elemental mapping result of Ni-Fe-P-Se to demonstrate the uniform distribution of Ni, Fe, P, Se, C, N, and O, which confirms the uniform growth of the Ni-Fe-P-Se composite.

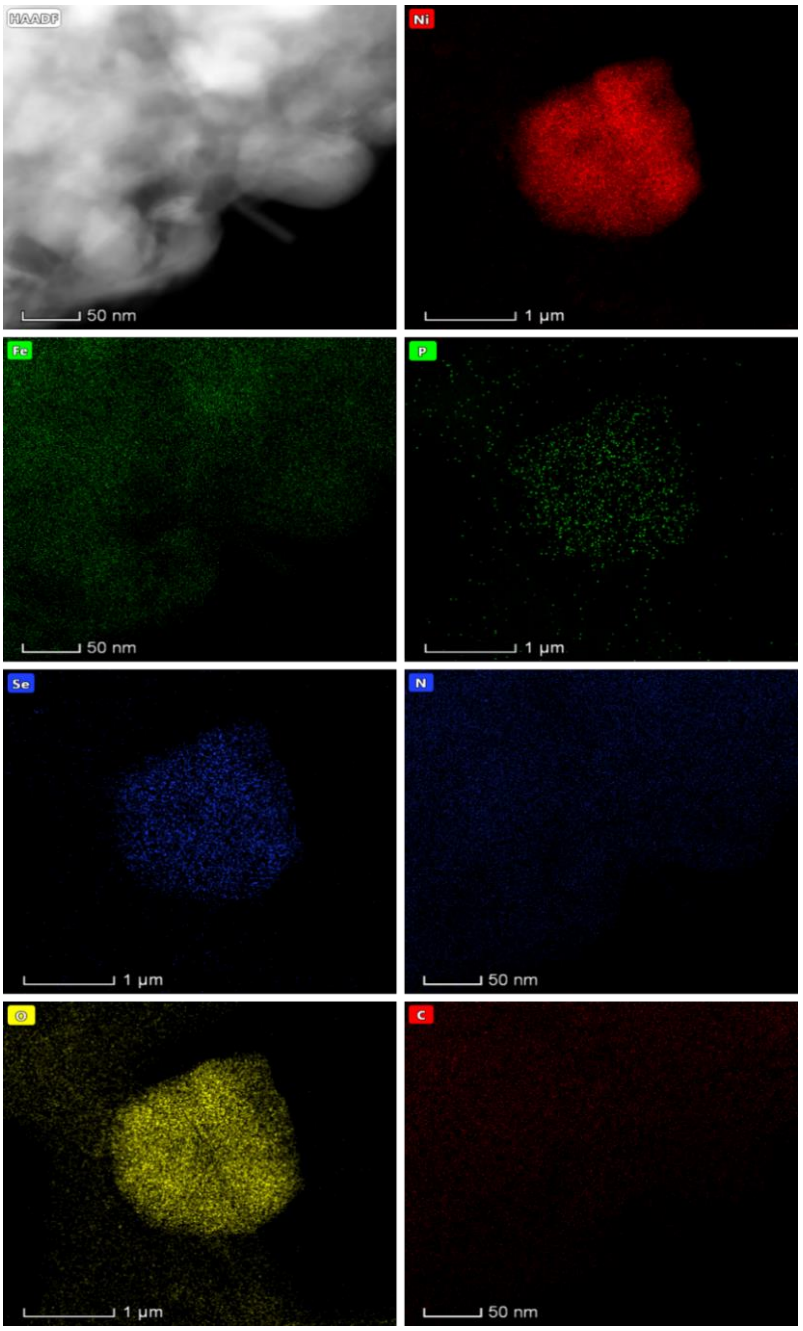


***Figure 5.*** *Elemental mapping of as-synthesized material (Ni-Fe-P-Se)*

Different morphology of electrocatalytic materials, as well as chemical composition, were studied *via* SEM. Average morphologies of the as-obtained Ni-P-Se, Fe-P-Se and Ni-Fe-P-Se were observed at different magnifications, as shown in Figure 6. It is observed that the Ni-P-Se shows the morphology on NF with its desired quantity, as depicted in Figure 6a. Figure 6b reveals the morphological aspects of Fe-P-Se, which is grown on NF as well. It can be seen that Fe-P-Se has an agglomerated lumpy structure. In Figure 6c, the morphology of Ni-Fe-P-Se can be seen, which shows a higher amount of prepared material on NF, with varied surface features than both previous samples of Ni-P-Se and Fe-P-Se, respectively. Through the SEM images, we have observed agglomerated surface features of various elements within the as-prepared Ni-Fe-P-Se structure as a potential composite for electrochemical water splitting application [34,35].

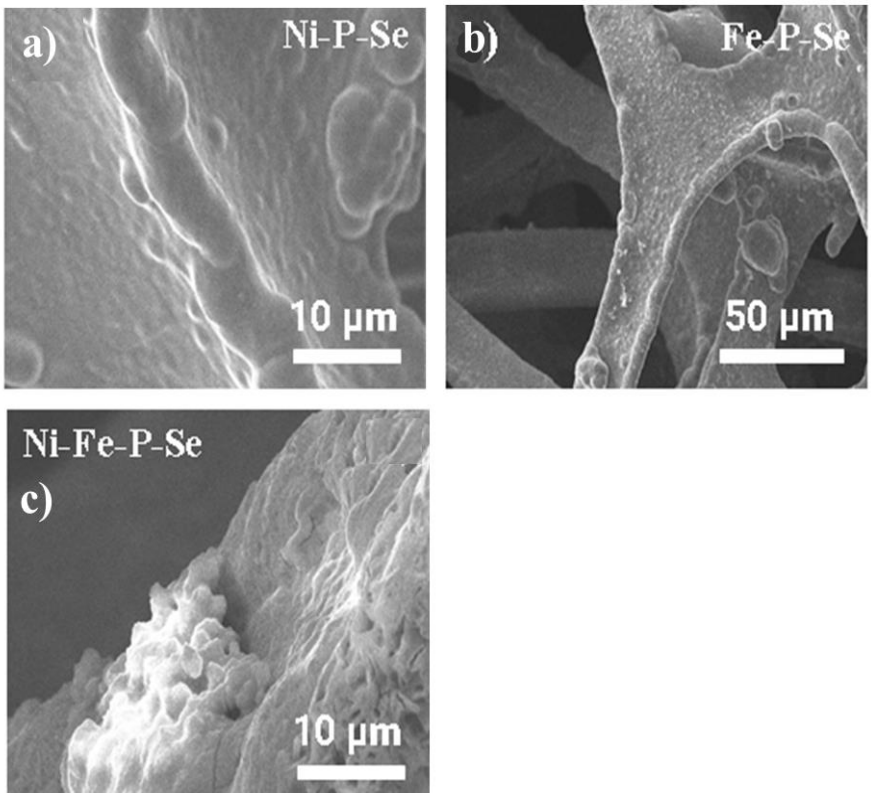


***Figure 6.*** *SEM images; (a) Ni-P-Se, (b) Fe-P-Se, and (c) Ni-Fe-P-Se*

*Electrochemical analysis*

The electrocatalytic HER performance on Ni-P-Se, Fe-P-Se, and Ni-Fe-P-Se was initially investigated in an alkaline electrolyte (1.0 M KOH) using LSV. Figure 7a exhibits the LSV curves of three proposed electrocatalysts with reference to a Pt-based electrocatalyst. It can be seen that the constructed Ni-Fe-P-Se has an activity for HER with a lower overpotential value of 316 mV at 10 mA $cm^{-2}$ as compared to other electrocatalysts (Ni-P-Se and Fe-P-Se) with overpotential values of 385 and 458 mV, respectively. Tafel slope has always been a crucial analysis tool in HER reaction kinetics for the determination of the rate-determining step [36-38]. The Tafel slope value of Ni-Fe-P-Se was calculated as 89 mV $dec^{-1}$, which is significantly lower than for the other two prepared electrocatalysts, computed as 162 and 138 mV $dec^{-1}$ for Ni-P-Se and Fe-P-Se, respectively. Based on the Tafel slope values, it should be discussed what HER mechanism is in question and which reaction step is rate-determining in each case (Tafel, Volmer or Heyrovsky). The HER mechanism for Tafel slopes for TMs involves the electrochemical reduction of protons to hydrogen gas on the surface of a transition metal catalyst. There are two categories of the HER mechanism: Volmer-Tafel and Heyrovsky mechanisms. Tafel slope has been expressed as the logarithmic derivative of the current density with respect to the applied potential. Figure 7 b shows the computed Tafel slope values for Ni-P-Se, Fe-P-Se, and Ni-Fe-P-Se, respectively.

Moreover, the stable and durable nature of an electrocatalyst is essential toward its practical usage [39]. Therefore, the stability of the as-prepared electrocatalyst (Ni-Fe-P-Se) was analysed through chronopotentiometry technique for 24 hours at the current density of 10 mA $cm^{-2}$, as shown in Figure 8a. It is observed that the Ni-Fe-P-Se has a strong, stable nature in terms of potential value, which showed a negligible change with time. Furthermore, durability is another important factor for the electro-catalyst, especially in $H_2$ production through electrocatalysis [40]. The stability of Ni-Fe-P-Se is tested through chronopotentiometry at 10 mA $cm^{-2}$ (Figure 8b), and durability before and after chronopotentiometry test,

as demonstrated in Figure 8c. The material (Ni-Fe-P-Se) showed a very durable behaviour for electrochemical HER in an alkaline medium without any major change in LSV curves. Such stable and durable behaviour of Ni-Fe-P-Se material supports this composite as a potential candidate for active HER response.

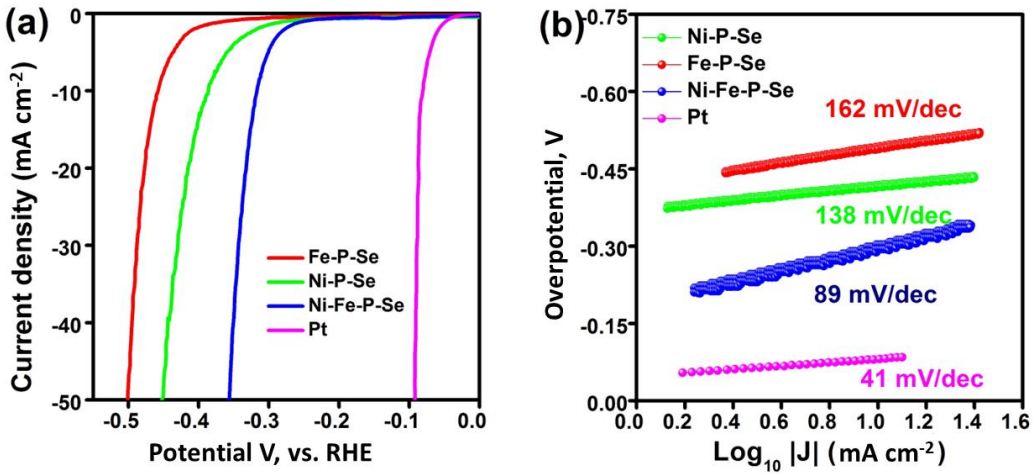


***Figure 7.*** *(a) Linear sweep voltammetry curves of Ni-P-Se, Fe-P-Se, Ni-Fe-P-Se, and Pt (as reference), (b) corresponding Tafel slopes*

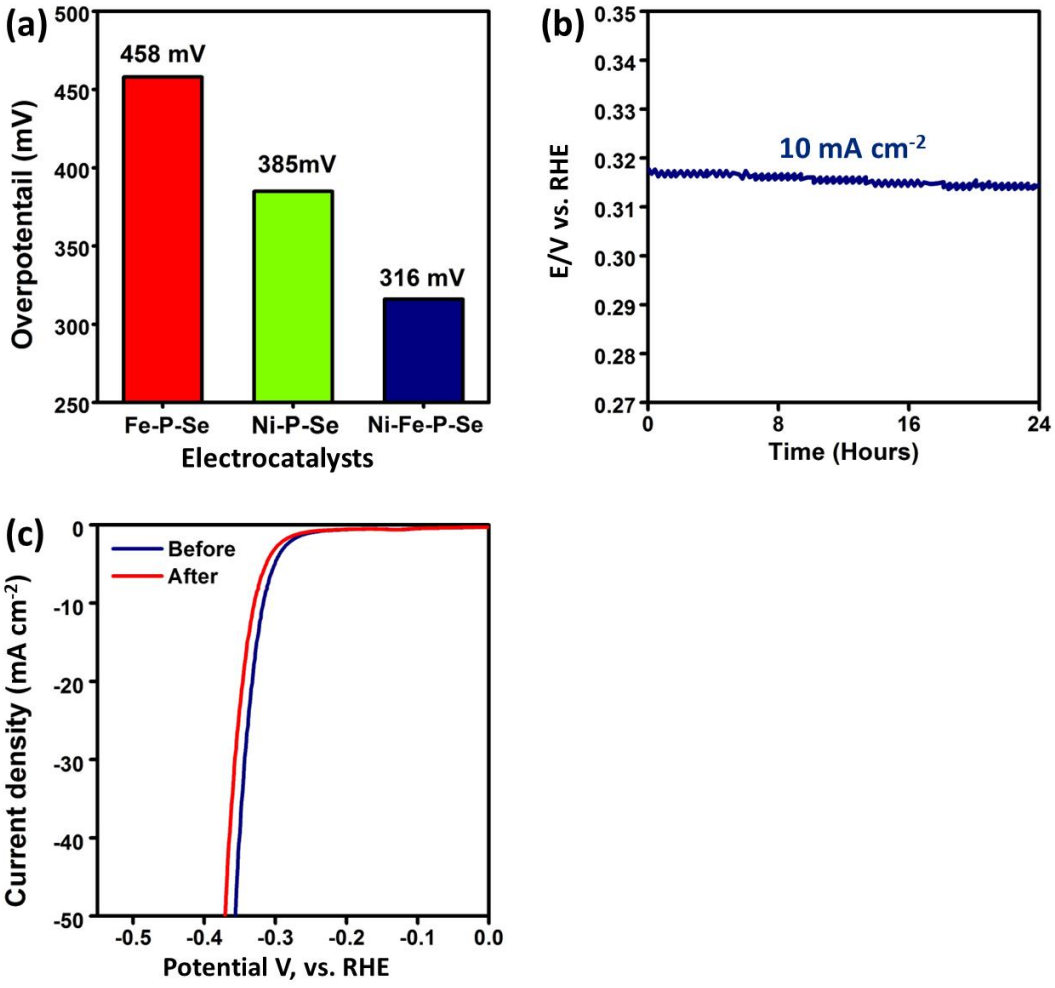


***Figure 8.*** *(a) Overpotential values at 10 mA cm$^{-2}$ of various electrocatalysts (b) chronopotentiometry test of Ni-Fe-P-Se for 24 hours at a current density of 10 mA cm$^{-2}$, (c) durability test of the as-prepared Ni-Fe-P-Se before and after chronopotentiometry test*

The corresponding overpotential values at 10 mA $cm^{-2}$ for every electrocatalyst material are shown in the form of histogram, as depicted in Figure 8a. The lower overpotential value, lower Tafel slope, and stable nature of Ni-Fe-P-Se have proven this composite as a comparable transition metal-based electrocatalyst appropriate for electrochemical applications in alkaline water splitting [41,42].

Figure 9 demonstrates the functioning of a current-time curve. Chemical reaction kinetics, diffusion processes, and adsorption are all studied using current-time analysis. This approach entails applying a quick shift in electric potential to the electrode and then observing the resulting current as a function of time [43,44]. It is shown that the greater the current, the straight the time, and its activity may preserve the efficiency of the device [44,45]. The corresponding current-time values of Ni-P-Se, Fe-P-Se, and Ni-Fe-P-Se can be seen in Figures 9a-9c). Using the parameters listed in Table 1, the current-time curves were created. After 600 to 1200 s of the water-splitting reaction, no corrosion on the electrodes could be seen in the plots.

***Table 1.*** *Experimental values for amperometry at sensitivity of* $10^{-6}$

| Reading | Initial V | Run time, s |
|---|---|---|
| 1 | 1.0 | 60 |
| 2 | 0.8 | 600 |
| 3 | 0.5 | 1200 |

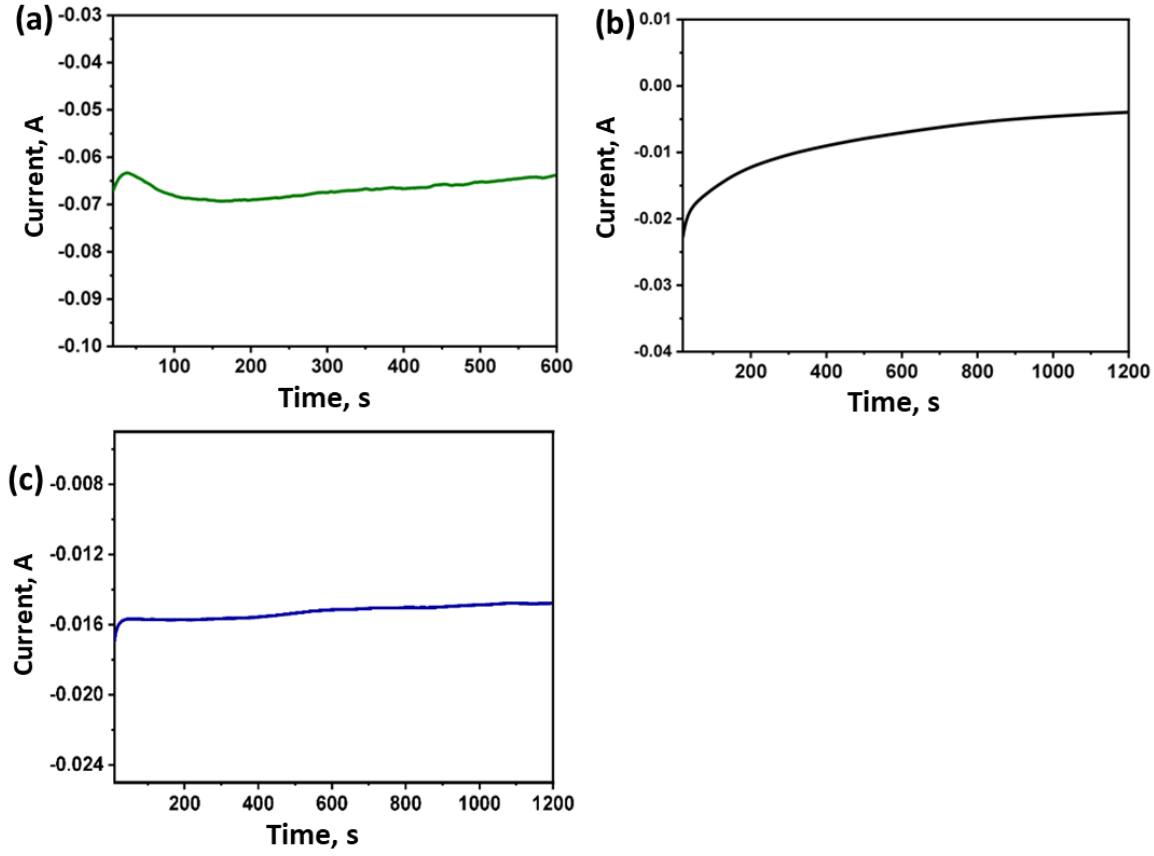


***Figure 9.*** *Current-time curve for: (a) Ni-P-Se, (b) Fe-P-Se, (c) Ni-Fe-P-Se*

## Conclusion

Ni-P-Se, Fe-P-Se, and Ni-Fe-P-Se solutions were effectively synthesized *via* a facile one-pot method. After the corresponding treatment, the prepared materials were deposited on the nickel foam by drop casting method. The XRD analysis of samples confirmed the crystallinity of different materials, including Ni-P-Se, Fe-P-Se, and Ni-Fe-P-Se. SEM showed the surface structure of these

materials with some modifications between them, while EDS confirmed the presence of various elements within as-prepared materials. According to the electrochemical analysis, Ni-Fe-P-Se exhibited much better catalytic activity for HER as compared with Ni-P-Se and Fe-P-Se, showing the overpotential value of 316 mV at 10 mA $cm^{-2}$, and 89 mV $dec^{-1}$ value of Tafel slope, respectively. The prepared electrocatalyst is stable for 24 hours at a current density value of 10 mA $cm^{-2}$. Such electrochemical features, including lower overpotential value, lower Tafel slope and high stability, suggest that this composed material based on Ni, Fe, P and Se is a robust electrocatalyst for $H_2$ production in alkaline media and energy conversion applications.

***Acknowledgments:*** *We express our gratitude and thanks to the financial support of the National Natural Science Foundation of China (NSFC 51402065 and 51603053), the Natural Science Foundation of Heilongjiang Province (LH2019E025), the Foundation Research Fund of Central University and Harbin Applied Technology Research and Development project (3072019CF1003), National Defence Industrial Technology Development program (JCKY2016604C006), and The National Key Research and Development Program of China (2016YFE0202700). We also express gratitude and thanks to the National Key Research and Development Program of China, Grant No. 2016YFF0102601, the "Strategic Priority Research Program" of the Institute of Process Engineering, Chinese Academy of Sciences.*

## References

[1] H. El Alami, J. Creus, X. Feaugas. Thermodynamic parameters evolution versus plastic strain during HER on nickel in sulphuric acid, *Electrochimica Acta* **52(12)** (2007) 4004-4014. https://doi.org/10.1016/j.electacta.2006.11.029

[2] A. Hanan, M. N. Lakhan, D. Shu, A. Hussain, M. Ahmed, I. A. Soomro, V. Kumar, D. Cao. An efficient and durable bifunctional electrocatalyst based on PdO and $Co_2FeO_4$ for HER and OER, *International Journal of Hydrogen Energy* **48(51)** (2023) 19494-19508. https://doi.org/10.1016/j.ijhydene.2023.02.049

[3] C. Hu, C. Lv, S. Liu, Y. Shi, J. Song, Z. Zhang, J. Cai, A. Watanabe, Nickel Phosphide Electrocatalysts for Hydrogen Evolution Reaction, *Catalysts* **10(2)** (2020) 188. https://doi.org/10.3390/catal10020188

[4] A. G. Maher, M. Liu, D. G. Nocera, Ligand Noninnocence in Nickel Porphyrins: Nickel Isobacteriochlorin Formation under Hydrogen Evolution Conditions, *Inorganic Chemistry* **58** (2019) 7958-7968. https://doi.org/10.1021/acs.inorgchem.9b00717

[5] A. Hanan, M. Ahmed, M.N. Lakhan, A.H. Shar, D. Cao, A. Asif, A. Ali, M. Gul, Novel rGO@$Fe_3O_4$ nanostructures: An active electrocatalyst for hydrogen evolution reaction in alkaline media *Journal of the Indian Chemical Society* **99(5)** (2022) 100442. https://doi.org/10.1016/j.jics.2022.100442

[6] Z. H. Ibupoto, A. Tahira, A.A. Shah, U. Aftab, M.Y. Solangi, J.A. Leghari, A.H. Samoon, A.L. Bhatti, M.A. Bhatti, R. Mazzaro, V. Morandi, M.I. Abro, A. Nafady, A.M. Al-Enizi, M. Emo, B. Vigolo, $NiCo_2O_4$ nanostructures loaded onto pencil graphite rod: An advanced composite material for oxygen evolution reaction, *International Journal of Hydrogen Energy* **47(10)** (2022) 6650-6665. https://doi.org/10.1016/j.ijhydene.2021.12.024

[7] U. Aftab, A. Tahira, A.H. Samo, M.I. Abro, M.M. Baloch, M. Kumar, Sirajuddin, Z.H. Ibupoto, Mixed $CoS_2$@$Co_3O_4$ composite material: An efficient nonprecious electrocatalyst for hydrogen evolution reaction, *International Journal of Hydrogen Energy* **45(27)** (2020) 13805-13813. https://doi.org/10.1016/j.ijhydene.2020.03.131

[8] B. Pierozynski, T. Mikolajczyk, I.M. Kowalski, Hydrogen evolution at catalytically-modified nickel foam in alkaline solution, *Journal of Power Sources* **271** (2014) 231-238. https://doi.org/10.1016/j.jpowsour.2014.07.188

[9] F. Song, W. Li, G. Han, Y. Sun, Electropolymerization of Aniline on Nickel-Based Electrocatalysts Substantially Enhances Their Performance for Hydrogen Evolution, *ACS Applied Energy Materials* **1(1)** (2018) 3-8. https://doi.org/10.1021/acsaem.7b00005

[10] A. Hanan, M.Y. Solangi, A. Jaleel laghari, A.A. Shah, U. Aftab, Z.A. Ibupoto, M.I. Abro, M.N. Lakhan, I.A. Soomro, E.A. Dawi, A. Al Karim, H. Ismail, E. Mustafa, B. Vigolo, A. Tahira, Z.H. Ibupoto, PdO@$CoSe_2$ composites: efficient electrocatalysts for water oxidation in alkaline media *RSC Advances* **13(1)** (2023) 743-755. http://doi.org/10.1039/D2RA07340D

[11] L. Wan, J. Zhang, Y. Chen, C. Zhong, W. Hu, Y. Deng, Varied hydrogen evolution reaction properties of nickel phosphide nanoparticles with different compositions in acidic and alkaline conditions, *Journal of Materials Science* **52** (2017) 804-814. http://doi.org/10.1007/s10853-016-0377-7

[12] F. Xiao, L. Li, W. Cui, Y. Zhang, C. Zhan, W. Xiao, Aligned porous nickel electrodes fabricated via ice templating with submicron particles for hydrogen evolution in alkaline water electrolysis, *Journal of Power Sources* **556** (2023) 232441. http://doi.org/10.1016/j.jpowsour.2022.232441

[13] W. Zhang, W. Li, Y. Li, S. Peng, Z. Xu, One-step synthesis of nickel oxide/nickel carbide/graphene composite for efficient dye-sensitized photocatalytic $H_2$ evolution, *Catalysis Today* **335** (2019) 326-332. http://doi.org/10.1016/j.cattod.2018.12.016

[14] M. Ahmed, M.N. Lakhan, Y. Tian, A.H. Shar, J. Yu, I. Ali, J. Liu, J. Wang, Fe (Pb)-P-Se nanocubes as her electrocatalysts for overall efficient water-splitting, *Digest Journal of Nanomaterials and Biostructures* **15(1)** (2020) 207-215. https://doi.org/10.15251/DJNB.2020.151.207

[15] Y. Pei, Y. Yang, F. Zhang, P. Dong, R. Baines, Y. Ge, H. Chu, P.M. Ajayan, J. Shen, M. Ye, Controlled Electrodeposition Synthesis of Co–Ni–P Film as a Flexible and Inexpensive Electrode for Efficient Overall Water Splitting, *ACS Applied Materials & Interfaces* **9(37)** (2017) 31887-31896. https://doi.org/10.1021/acsami.7b09282

[16] H. Xu, J. Zhu, P. Wang, D. Chen, C. Zhang, M. Xiao, Q. Ma, H. Bai, R. Qin, J. Ma, S. Mu, Fe–Co–P multi-heterostructure arrays for efficient electrocatalytic water splitting, *Journal of Materials Chemistry A* **9(43)** (2021) 24677-24685. https://doi.org/10.1039/D1TA06603J

[17] X. Xing, C. Wu, G. Yang, T. Tong, Y. Wang, D. Wang, F.C. Robles Hernandez, Z. Ren, Z. Wang, J. Bao, $FeSe_2$/CoSe nanosheets for efficient overall water splitting under low cell voltages *Materials Today Chemistry* **26** (2022) 101110. https://doi.org/10.1016/j.mtchem.2022.101110

[18] I.H. Kwak, H.S. Im, D.M. Jang, Y.W. Kim, K. Park, Y.R. Lim, E.H. Cha, J. Park, $CoSe_2$ and $NiSe_2$ Nanocrystals as Superior Bifunctional Catalysts for Electrochemical and Photoelectrochemical Water Splitting, *ACS Applied Materials & Interfaces* **8(8)** (2016) 5327-5334. https://doi.org/10.1021/acsami.5b12093

[19] A.Hanan Samo, U. Aftab, M. Yameen, A.J. Laghari, M. Ahmed, M.N. Lakhan, A.H. Shar, A. Ali, A. Ali, A magnesium doped cobalt-oxide composite for active oxygen evolution reaction, *Journal of Applied and Emerging Sciences* **11(2)** (2021) 210-216. https://doi.org/10.36785/JAES.112519

[20] A. Hanan, D. Shu, U. Aftab, D. Cao, A.J. Laghari, M.Y. Solangi, M.I. Abro, A. Nafady, B. Vigolo, A. Tahira, and Z.H. Ibupoto, $Co_2FeO_4$@rGO composite: Towards trifunctional water splitting in alkaline media, *International Journal of Hydrogen Energy* **47(80)** (2022) 33919-33937. https://doi.org/10.1016/j.ijhydene.2022.07.269

[21] D. Han, G. Du, Y. Wang, L. Jia, W. Zhao, Q. Su, S. Ding, M. Zhang, B. Xu, Chemical Energy-Driven Lithiation Preparation of Defect-Rich Transition Metal Nanostructures for Electrocatalytic Hydrogen Evolution, *Small* **18(35)** (2022) 2202779. https://doi.org/10.1002/smll.202202779

[22] Z. Zhu, H. Yin, C.-T. He, M. Al-Mamun, P. Liu, L. Jiang, Y. Zhao, Y. Wang, H.-G. Yang, Z. Tang, D. Wang, X.-M. Chen, H. Zhao, Ultrathin Transition Metal Dichalcogenide/3d Metal Hydroxide Hybridized Nanosheets to Enhance Hydrogen Evolution Activity, *Advanced Materials* **30(28)** (2018) 1801171. https://doi.org/10.1002/adma.201801171

[23] M.J. Gomez, E.A. Franceschini, G.I. Lacconi, Ni and $Ni_xCo_y$Alloys Electrodeposited on Stainless Steel AISI 316L for Hydrogen Evolution Reaction, *Electrocatalysis* **9** (2018) 459-470. https://doi.org/10.1007/s12678-018-0463-5

[24] M.A. Ruiz Fresneda, J. Delgado Martín, J. Gómez Bolívar, M.V. Fernández Cantos, G. Bosch-Estévez, M.F. Martínez Moreno, M.L. Merroun, Green synthesis and biotransformation of amorphous Se nanospheres to trigonal 1D Se nanostructures: impact on Se mobility within the concept of radioactive waste disposal, *Environmental Science: Nano* **5** (2018) 2103-2116. https://doi.org/10.1039/C8EN00221E

[25] J.T. Richardson, R. Scates, M.V. Twigg, X-ray diffraction study of nickel oxide reduction by hydrogen, *Applied Catalysis A: General* **246(1)** (2003) 137-150. https://doi.org/10.1016/S0926-860X(02)00669-5

[26] H. Wang, X. Kou, J. Zhang, J. Li, Large scale synthesis and characterization of Ni nanoparticles by solution reduction method, *Bulletin of Materials Science* **31** (2008) 97-100. https://doi.org/10.1007/s12034-008-0017-1

[27] K. He, F.-X. Ma, C.-Y. Xu, J. Cumings, Mapping magnetic fields of $Fe_3O_4$ nanosphere assemblies by electron holography, *Journal of Applied Physics* **113(17)** (2013) 17B528. https://doi.org/10.1063/1.4798500

[28] R.S. Sahu, R.-a. Doong, Functionalized Fe/Ni@g-C3N4 nanostructures for enhanced trichloroethylene dechlorination and successive oxygen reduction reaction activity *Environmental Science: Nano* **7** (2020) 3469-3481. https://doi.org/10.1039/D0EN00450B

[29] X. Liang, B. Zheng, L. Chen, J. Zhang, Z. Zhuang, B. Chen, MOF-Derived Formation of $Ni_2P$-CoP Bimetallic Phosphides with Strong Interfacial Effect toward Electrocatalytic Water Splitting, *ACS Applied Materials & Interfaces* **9(27)** (2017) 23222-23229. https://doi.org/10.1021/acsami.7b06152

[30] H. Zhang, H. Tang, Q. Weng, Q. Wei, M. Duan, X. Bo, F. Fu, L. Zan. Engineering heterostructure of bimetallic nickel-silver sulfide as an efficient electrocatalyst for overall water splitting in alkaline media, *Journal of Solid State Chemistry* **316** (2022) 123556. https://doi.org/10.1016/j.jssc.2022.123556

[31] L.P. Hao, A. Hanan, R. Walvekar, M. Khalid, F. Bibi, W.Y. Wong, C. Prakash, Synergistic Integration of MXene and Metal-Organic Frameworks for Enhanced Electrocatalytic Hydrogen Evolution in an Alkaline Environment, *Catalysts* **13(5)** (2023) 802. https://doi.org/10.3390/catal13050802

[32] H. Zhang, S. Geng, M. Ouyang, H. Yadegari, F. Xie, D.J. Riley. A Self-Reconstructed Bifunctional Electrocatalyst of Pseudo-Amorphous Nickel Carbide @ Iron Oxide Network for Seawater Splitting, *Advanced Science* **9(15)** (2022) 2200146. https://doi.org/10.1002/advs.202200146

[33] D. Liu, D. Li, D. Yang, Size-dependent magnetic properties of branchlike nickel oxide nanocrystals, *AIP Advances* **7** (2017) 015028. https://doi.org/10.1063/1.4974307

[34] M.Y. Solangi, A.H. Samo, A.J. Laghari, U. Aftab, M.I. Abro, M.I. Irfan, $MnO_2$@$Co_3O_4$ nanocomposite based electrocatalyst for effective oxygen evolution reaction, *Sukkur IBA Journal of Emerging Technologies (SJET)* **5** (2022) 32-40. https://doi.org/10.30537/sjet.v5i1.958

[35] Y. Hong, C.H. Choi, S.-I. Choi, Catalytic Surface Specificity of $Ni(OH)_2$-Decorated Pt Nanocubes for the Hydrogen Evolution Reaction in an Alkaline Electrolyte, *ChemSusChem* **12(17)** (2019) 4021-4028. https://doi.org/10.1002/cssc.201901539

[36] A. Samo, U. Aftab, D. Cao, M. Ahmed, M. Lakhan, V. Kumar, A. Asif, A. Ali, Schematic synthesis of cobalt-oxide ($Co_3O_4$) supported cobalt-sulfide (CoS) composite for oxygen evolution reaction, *Digest Journal of Nanomaterials and Biostructures* **17(1)** (2022) 109-120. https://doi.org/10.15251/DJNB.2022.171.109

[37] A. Hanan, A.J. Laghari, M.Y. Solangi, U. Aftab, M.I. Abro, D. Cao, M. Ahmed, M.N. Lakhan, A. Ali, and A. Asif, $CdO/Co_3O_4$ Nanocomposite as an Efficient Electrocatalyst for Oxygen Evolution Reaction in Alkaline Media, *International Journal of Engineering Science Technologies* **6(1)** (2022) 1-10. https://doi.org/10.29121/IJOEST.v6.i1.2022.259

[38] A.J. Laghari, U. Aftab, A. Tahira, A.A. Shah, A. Gradone, M.Y. Solangi, A.H. Samo, M. kumar, M.I. Abro, M.w. Akhtar, R. Mazzaro, V. Morandi, A.M. Alotaibi, A. Nafady, A. Infantes-Molina, Z.H. Ibupoto, MgO as promoter for electrocatalytic activities of $Co_3O_4$–MgO composite via abundant oxygen vacancies and $Co^{2+}$ ions towards oxygen evolution reaction *International Journal of Hydrogen Energy* **48** (2023) 12672-12682. https://doi.org/10.1016/j.ijhydene.2022.04.169

[39] S. Balu, A. Hanan, H. Venkatesvaran, S.-W. Chen, T.C.-K. Yang, M.J.C. Khalid, Recent Progress in Surface-Defect Engineering Strategies for Electrocatalysts toward Electrochemical $CO_2$ Reduction: A Review, *Catalysts* **13(2)** (2023) 393. https://doi.org/10.3390/catal13020393

[40] R.R. Raja Sulaiman, A. Hanan, W.Y. Wong, R.M. Yunus, K.S. Loh, R. Walvekar, V. Chaudhary, M.J.C. Khalid, Structurally Modified MXenes-Based Catalysts for Application in Hydrogen Evolution Reaction: A Review, *Catalysts* **12(12)** (2022) 1576. https://doi.org/10.3390/catal12121576

[41] D. Escalera-López, R. Griffin, M. Isaacs, K. Wilson, R.E. Palmer, N.V. Rees, Electrochemical sulfidation of $WS_2$ nanoarrays: Strong dependence of hydrogen evolution activity on transition metal sulfide surface composition, *Electrochemistry Communications* **81** (2017) 106-111. https://doi.org/10.1016/j.elecom.2017.06.016

[42] Y. Zhu, Q. Lin, Y. Zhong, H.A. Tahini, Z. Shao, H. Wang. Metal oxide-based materials as an emerging family of hydrogen evolution electrocatalysts, *Energy & Environmental Science* **13** (2020) 3361-3392. https://doi.org/10.1039/d0ee02485f

[43] A. Ali, F. Long, P.K. Shen. Innovative Strategies for Overall Water Splitting Using Nanostructured Transition Metal Electrocatalysts, *Electrochemical Energy Reviews* **5** (2022) 1. https://doi.org//10.1007/s41918-022-00136-8

[44] J. Hu, C. Zhang, Y. Zhang, B. Yang, Q. Qi, M. Sun, F. Zi, M.K.H. Leung, B. Huang, Interface Modulation of $MoS_2$/Metal Oxide Heterostructures for Efficient Hydrogen Evolution Electrocatalysis, *Small* **16** (2020) 2002212. https://doi.org/10.1002/smll.202002212

[45] A.Q. Mugheri, A.A. Otho, A.A. Mugheri, Meritorious spatially on hierarchically $Co_3O_4/MoS_2$ phase nanocomposite synergistically a high-efficient electrocatalyst for hydrogen evolution reaction performance: Recent advances & future perspectives, *International Journal of Hydrogen Energy* **46** (2021) 22707-22718. https://doi.org/10.1016/j.ijhydene.2021.04.122